

Circumstellar properties of Type Ia supernovae from the helium star donor channel

Takashi J. Moriya,¹[★] Dongdong Liu,^{2,3,4,5} Bo Wang^{2,3,4,5} and Zheng-Wei Liu^{2,3,4,5}

¹*Division of Science, National Astronomical Observatory of Japan, National Institutes of Natural Sciences, 2-21-1 Osawa, Mitaka, Tokyo 181-8588, Japan*

²*Yunnan Observatories, Chinese Academy of Sciences, Kunming 650216, China*

³*Key Laboratory for the Structure and Evolution of Celestial Objects, Chinese Academy of Sciences, Kunming 650216, China*

⁴*University of Chinese Academy of Sciences, Beijing 100049, China*

⁵*Centre for Astronomical Mega-Science, Chinese Academy of Sciences, Beijing 100012, China*

Accepted 2019 July 06. Received 2019 July 06; in original form 2019 April 09

ABSTRACT

We investigate predicted circumstellar properties of Type Ia supernova progenitor systems with non-degenerate helium star donors. It has been suggested that systems consisting of a carbon+oxygen white dwarf and a helium star can lead to Type Ia supernova explosions. Binary evolution calculations for the helium star donor channel predict that such a progenitor system is in either a stable helium-shell burning phase or a weak helium-shell flash phase at the time of the Type Ia supernova explosion. By taking the binary evolution models from our previous study, we show that a large fraction of the progenitor systems with a helium star donor have low enough density to explain the current non-detection of radio emission from Type Ia supernovae. Most of the progenitor systems in the weak helium-shell flash phase at the time of the Type Ia supernova explosions, which may dominate the prompt (short delay time) Type Ia supernova population, have both low circumstellar density and a faint helium star donor to account for the non-detection of radio emission and a pre-explosion companion star in SN 2011fe and SN 2014J. We also find some progenitor systems that are consistent with the properties of the companion star candidate identified at the explosion location of Type Iax SN 2012Z.

Key words: binaries: close – circumstellar matter – stars: evolution – supernovae: general – supernovae: individual (SN 2011fe, SN 2014J, SN 2012Z) – white dwarfs

1 INTRODUCTION

Type Ia supernovae (SNe) are suggested to be thermonuclear explosions of C+O white dwarfs (WDs, e.g., Hoyle & Fowler 1960), which is recently confirmed observationally (Nugent et al. 2011; Bloom et al. 2012). Despite of their uniformity that led to the discovery of the accelerating expansion of the Universe (Riess et al. 1998; Perlmutter et al. 1999), there are diverse theories for their progenitors and explosion mechanisms (see Maoz et al. 2014; Maeda & Terada 2016; Livio & Mazzali 2018; Wang 2018 for recent reviews).

One big question in SN Ia progenitors is the nature of their companion stars. The canonical model of SNe Ia requires C+O WDs to grow their mass near the Chandrasekhar limit to trigger thermonuclear explosions (e.g., Thielemann et al. 2004). The nature of the donor stars is,

however, largely debated. One possible donor star is a non-degenerate star (the single-degenerate (SD) model; e.g., Nomoto 1982a; Whelan & Iben 1973). The non-degenerate star can transfer its mass to the WD so that the WD can burn the transferred mass on its surface to grow its mass. Another possibility is that the companion star is also a WD (the double-degenerate (DD) model; e.g., Webbink 1984; Iben & Tutukov 1984). The companion WD itself could be a donor star enabling a stable burning (e.g., Bildsten et al. 2007) or two WDs merge after losing their orbital energy through gravitational waves. The merger itself may trigger a SN Ia explosion (e.g., Pakmor et al. 2012) or a disrupted WD during the merger may be accreted to the survived WD to make it grow near the Chandrasekhar limit (e.g., Dan et al. 2014; Shen 2015; Sato et al. 2016; Liu et al. 2018; Mori et al. 2019). However, the later case is usually considered to end up with accretion-induced collapse (AIC) of WDs rather than SN Ia explosions (e.g., Nomoto & Iben 1985; Saio & Nomoto 1985, but see also Yoon et al. 2007).

[★] E-mail: takashi.moriya@nao.ac.jp (TJM)

Many observational attempts have been made to constrain the companion stars. One method often used is radio and X-ray observations. The SD model is predicted to have much denser circumstellar media (CSM) than the DD model because of the mass transfer required to grow WDs. The interaction between SN ejecta and a CSM results in radio and X-ray emission through which we can constrain CSM properties around SNe (e.g., [Chevalier 1998](#); [Chevalier & Fransson 2006](#); [Maeda 2012](#)). Especially, many attempts have been made to observe SNe Ia in radio but no radio signals have been detected from SNe Ia ([Chomiuk et al. 2014, 2016](#); [Horesh et al. 2012](#); [Pérez-Torres et al. 2014](#) and references therein). These radio observations exclude most of CSM properties predicted by the SD model with H-rich star donors and they are proposed to favor the DD model, although the SD H-rich star donor model also has a way to make a low CSM density environment if rotation of accreting WDs and their spin-down time are taken into account (e.g., [Justham 2011](#)).

Although observations have been mainly compared with the SD model with H-rich star donors, it has been suggested that accretion from non-degenerate He donor stars can also make the accompanying WDs to reach near the Chandrasekhar limit (e.g., [Iben & Tutukov 1994](#); [Yoon & Langer 2003](#); [Wang et al. 2009a](#); [Brooks et al. 2016](#); [?; Wong & Schwab 2019](#); [Neunteufel et al. 2019](#)). Especially, population synthesis models generally predict that SNe Ia from the SD He star donor channel are likely dominant in the prompt (short delay time) population of SNe Ia (e.g., [Wang et al. 2009b](#); [Ruiter et al. 2009](#); [Claeys et al. 2014](#); [Liu et al. 2015a](#)). WDs with He star donors have also been related to peculiar kinds of thermonuclear SNe such as SN 2002cx-like (a.k.a. Type Iax) SNe ([Foley et al. 2013](#) and references therein) and a possible He star donor has been identified in the pre-explosion image of a SN Iax 2012Z ([McCully et al. 2014](#); [Stritzinger et al. 2015](#); [Yamanaka et al. 2015](#)).

In the previous studies investigating CSM properties of SNe Ia, CSM properties expected from the SD He donor channel have not been considered much. Here, we investigate its CSM properties based on a grid of He star donor SN Ia progenitor models computed by [Wang et al. \(2009a\)](#). We compare our results with the previous constraints on the SN Ia CSM properties and show that most of the He star donor progenitors are hard to be excluded even with the current deepest radio observations.

The rest of this paper is organized as follows. We first introduce the binary evolution model of [Wang et al. \(2009a\)](#) which we use in this study in Section 2. We estimate the CSM properties around He star donor systems at the time of SN Ia explosions in Section 3. We compare the results with observations and have general discussion on the He star donor model for SNe Ia in Section 4. We conclude this paper in Section 5.

2 BINARY EVOLUTION MODEL

We adopt the binary evolution models of [Wang et al. \(2009a\)](#) in this study. We refer to [Wang et al. \(2009a\)](#) for the full details of the assumptions in the stellar and binary evolution calculations and we only briefly summarize them

here. [Wang et al. \(2009a\)](#) followed the binary evolution of about 2600 C+O WD + He star systems to identify the systems leading to SNe Ia. A SN Ia explosion is assumed to occur when the mass of the C+O WD in a system reaches $1.378 M_{\odot}$. The Eggleton’s stellar evolution code ([Eggleton 1971, 1972, 1973](#); [Han et al. 1994](#); [Pols et al. 1995, 1998](#)) is used to compute the stellar evolution in binary systems. Briefly, the Roche-lobe overflow is treated by the method described in [Han et al. \(2000\)](#). Mixing length theory is adopted with the Schwarzschild criteria with the mixing length parameter of 2.0. No overshooting is considered. The He stars are originally composed of He abundance of $Y = 0.98$ with the solar metallicity ($Z = 0.02$). The structure of WDs is not solved in the binary evolution calculation and the WD mass growth rate is set by the mass transfer rate. WDs about to explode as SNe Ia from the He star donor channel are expected to be in one of the following three burning phases: (1) the optically thick wind phase, (2) the stable He-shell burning phase, and (3) the weak He-shell flash phase.

The first important physical property determining the mass growth rate is the maximum He accretion rate that a WD can burn on the surface. It is $\dot{M}_{\max} \simeq 7.2 \times 10^{-6} (M_{\text{WD}}/M_{\odot} - 0.6) M_{\odot} \text{ yr}^{-1}$, where M_{WD} is the accreting WD mass ([Nomoto 1982b](#)). When the mass transfer rate becomes larger than this critical rate, the WD cannot burn all the transferred He and a He envelope is formed on top of the WD. This phase is called “optically thick wind phase” and we assume the extended He envelope results in the so-called “optically thick wind” (e.g., [Kato & Hachisu 1994](#); [Hachisu et al. 1996](#)). The WD mass grows with \dot{M}_{\max} in this phase.

If the He accretion rate onto the WD is less than \dot{M}_{\max} but above the minimum stable He burning accretion rate (\dot{M}_{st} , see [Kato & Hachisu 2004](#)), all the accreted He is burned at the WD surface and the WD mass grows steadily with the mass transfer rate. When the He accretion rate goes below \dot{M}_{st} , the He shell flash occurs at the WD surface. If the accretion rate is below \dot{M}_{st} but above the weak He-shell flash accretion limit ($4.0 \times 10^{-8} M_{\odot} \text{ yr}^{-1}$, [Woosley et al. 1986](#)), the He flash is “weak” and a part of the shell is ejected from the system. The WD mass can still grow in this phase with the rate estimated by [Kato & Hachisu \(2004\)](#). When the mass transfer rate becomes lower than the weak He-shell flash accretion limit, the He-shell flash becomes violent enough to prevent the WD mass growth. The WD mass does not increase in this case.

Although [Wang et al. \(2009a\)](#) assumed that the WDs at the optically thick wind phase explode as SNe Ia, [Wang et al. \(2017\)](#) later found that O+Ne+Mg WDs are usually formed during the optically thick wind phase and they do not explode as SNe Ia. These O+Ne+Mg WDs end up with AIC (e.g., [Nomoto & Kondo 1991](#)) rather than SN Ia explosions. Because such a system leading to AIC is considered to explode as SNe Ia in the original models in [Wang et al. \(2009a\)](#), we also show their CSM properties for reference in this study.

3 CIRCUMSTELLAR PROPERTIES

The two essential parameters in estimating the CSM property of each system are its mass-loss rate and wind velocity.

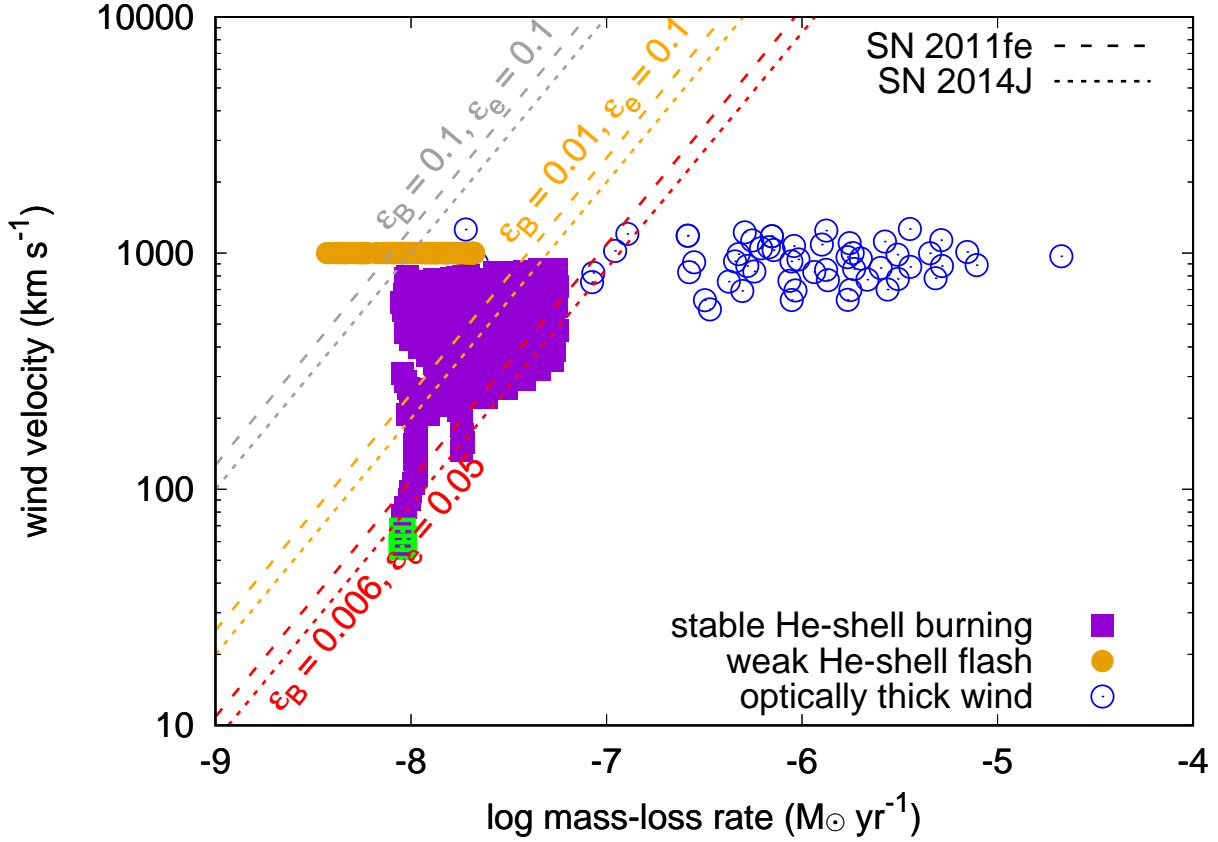


Figure 1. Mass-loss rates and wind velocities of SN Ia progenitors with He star donors. The burning phase of each system is indicated by the symbols. The observational constraints on the CSM properties from SN 2011fe and SN 2014J are shown with lines with three different microphysics (ϵ_B and ϵ_e) assumptions. The right side region of the lines is excluded by the radio observations. The models surrounded by green are those consistent with the companion star of SN 2012Z as shown in Fig. 2.

In this section, we present how we estimate the mass-loss rate and wind velocity from each system from the binary evolution model introduced in the previous section. The way we use to estimate the mass-loss rates and wind velocities depends on in which phase the system is at the time of the SN Ia explosions.

3.1 Stable He-shell burning phase

If the system is in the stable He-shell burning phase, the accreted mass onto the WD from the He donor is all steadily burned on the surface of the WD. No mass loss is expected from the system in our binary evolution calculations. In reality, however, a small fraction of transferred mass is likely to escape from the system from the outer Lagrangian point (e.g., Huang & Yu 1996; Deufel et al. 1999). We assume that 1% of the transferred mass will be lost through the outer Lagrangian point (Huang & Yu 1996). We note that mass loss from the outer Lagrangian point leads to orbital shrinking of binary systems and, therefore, may result in a different evolution. However, we do not take such a difference into account in this work, partly because of the uncertain fraction of mass lost through the outer Lagrangian point. Especially, such a mass loss could change the initial binary parameter range of binary systems leading to SN Ia explosions

during the stable He-shell burning phase. Under these assumptions, the mass-loss rates are estimated to be between $\sim 10^{-8} M_{\odot} \text{ yr}^{-1}$ and $\sim 10^{-7} M_{\odot} \text{ yr}^{-1}$ (Fig. 1), because the mass transfer rates of the systems in this phase at the time of the SN Ia explosions are between $\sim 10^{-6} M_{\odot} \text{ yr}^{-1}$ and $\sim 10^{-5} M_{\odot} \text{ yr}^{-1}$ in our binary evolution models.

The wind velocity of the mass lost through the outer Lagrangian point is also not simply determined. The reasonable assumption is that the mass lost from the outer Lagrangian point acquires the orbital velocity there. The outer Lagrangian mass loss with the wind velocities of up to around 600 km s^{-1} , which are of the order of the orbital velocity, has been indeed seen in the P-Cygni profiles of stable nuclear burning WDs (Deufel et al. 1999). Therefore, we assume that the wind velocity in this phase is the same as the orbital velocity at the outer Lagrangian point. They are of the order of 100 km s^{-1} . It is also likely that the wind velocity decreases by the gravitational attraction. The earliest radio observation of SNe Ia to constrain the CSM properties has been performed at 1 day after the explosion (Chomiuk et al. 2016). The forward shock is at around 10^{14} cm at this epoch, while the outer Lagrangian point is at around 10^{11} cm . In such a case, the wind velocity could be reduced by a factor of ≈ 30 .

The mass-loss rates and wind velocities obtained in this

way are summarized in Fig. 1. The progenitor systems in this phase has relatively low mass-loss rates ($\sim 10^{-7} M_{\odot} \text{ yr}^{-1}$) with the wind velocity of the order of $\sim 100 \text{ km s}^{-1}$ or less.

3.2 Weak He-shell flash phase

The mass loss in the weak He-shell flash phase is triggered by the He-burning shell flash at the surface of the WD. The flash is not strong enough to reduce the WD mass and it grows. A small amount of mass is blown from the system. The mass growth rate of a WD in this phase is estimated by using the prescription of Kato & Hachisu (2004) in the binary evolution model. The difference between the mass transfer rate and the mass growth rate is assumed to be ejected from the system as a wind. The mass-loss rates are found to be between $\approx 3 \times 10^{-9} M_{\odot} \text{ yr}^{-1}$ and $\approx 3 \times 10^{-8} M_{\odot} \text{ yr}^{-1}$ (Fig. 1).

Because the weak He-shell flash is triggered by the nuclear burning at the surface of the accreting WD, we assume that the wind velocity becomes similar to those of novae. Yaron et al. (2005) estimate that nova ejecta from a $1.4 M_{\odot}$ WD have velocities of around 1000 km s^{-1} when the mass accretion rate is $10^{-7} - 10^{-6} M_{\odot} \text{ yr}^{-1}$, which matches with our models. Therefore, we simply assume that the wind velocity is 1000 km s^{-1} in this study.

The CSM properties estimated in this way are summarized in Fig. 1. The systems in the weak He-shell flash phase have relatively low CSM density due to the small mass-loss rates and the large wind velocities.

Although we assume a smooth wind in constraining the CSM properties, the shell flash can actually form a CSM with many shells (e.g., Chomiuk et al. 2012). Then, the CSM around SN Ia progenitors in the weak He-shell flash phase likely has a less dense component than we find in Fig. 1 between the shells. Such a shell-like structure can also exist around SN Ia progenitors with H-rich donor stars (Chomiuk et al. 2012).

3.3 Optically thick wind phase

We assume that the transferred mass that exceeds the critical mass accretion rate is ejected from the system as an optically thick wind when a system is in the optically thick wind phase. The mass-loss rates of the systems in the optically thick wind phase mostly exceed $10^{-7} M_{\odot} \text{ yr}^{-1}$ (Fig. 1). With the high accretion rate and strong He-shell burning, the WD would form an extended He envelope reaching the Roche lobe. We assume that the mass loss occurs around the Roche radius and the wind velocity would be the escape velocity from the He envelope extended to the Roche lobe radius. Then, the wind velocity becomes around 1000 km s^{-1} (Fig. 1).

4 DISCUSSION

4.1 Comparison with SN 2011fe and SN 2014J

The expected CSM properties for the He star donor channel of SNe Ia based on the binary evolution model of Wang et al. (2009a) are summarized in Fig. 1. The CSM properties around SNe Ia are well constrained by radio observations of

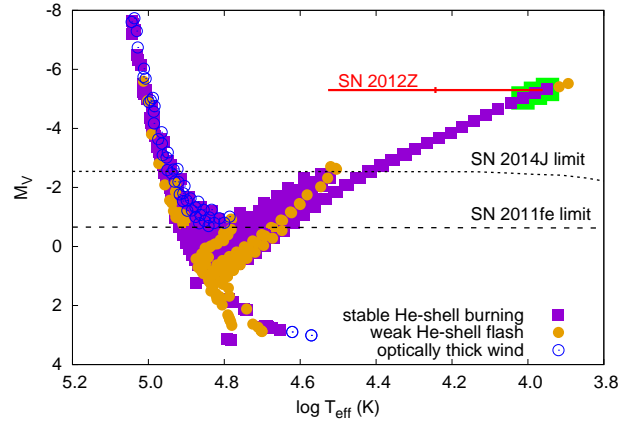


Figure 2. Effective temperature (T_{eff}) and absolute V band magnitude (M_V) of He star donors at the time of SN Ia explosions. The effective temperature is obtained by the binary evolution calculation. M_V is estimated by taking the bolometric luminosity obtained by the binary evolution model and applying the bolometric correction of Torres (2010). The same method is applied by Li et al. (2011). The M_V limits for SN 2011fe (Li et al. 2011) and SN 2014J (Kelly et al. 2014) are shown. The companion star of the SN 2012Z progenitor reported by McCully et al. (2014) is shown and the models consistent with it are marked with green.

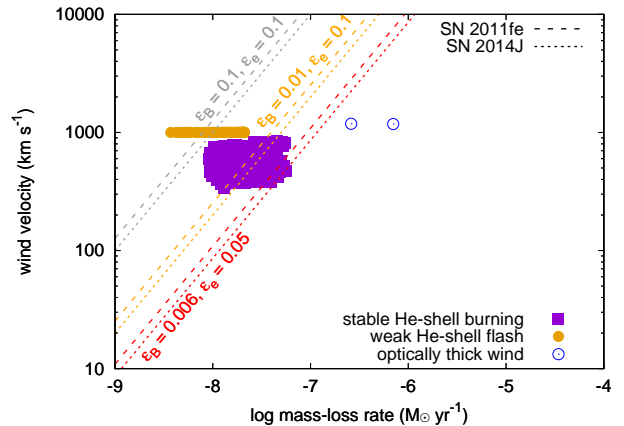


Figure 3. The same as Fig. 1, but only for those with He donor luminosity below the limit of SN 2011fe in Fig. 2.

SNe Ia (see Chomiuk et al. 2016 for a summary). No radio signals from SNe Ia have been observed so far. The deepest constraints on the CSM density around SNe Ia come from SN 2011fe (Chomiuk et al. 2012; Horesh et al. 2012) and SN 2014J (Pérez-Torres et al. 2014; Chomiuk et al. 2014; Chandler & Marvil 2014), which give the upper limits for the CSM density in Fig. 1. The right-side region of the lines are excluded by the radio observations.

Radio emission from SNe Ia originates from synchrotron emission from relativistic electrons accelerated at the shock wave between the SN ejecta and CSM. However, the microphysics at a shock wave is quite uncertain. For example, a fraction of kinetic energy injected to the shock wave that is converted to magnetic field (ϵ_B) and a fraction that is used to the relativistic electron acceleration (ϵ_e) are still not well constrained, although they play a very important role in es-

timating radio emission from SNe Ia. If we assume that the power-law index of the relativistic electron number density (p) is 3 and the outer density structure of SN Ia ejecta is proportional to r^{-7} , the CSM density constraint becomes proportional to $(\varepsilon_B \varepsilon_e)^{-0.7}$ (e.g., [Moriya et al. 2013](#)).

The CSM density constraints with three different combinations of ε_B and ε_e are shown in Fig. 1. ε_B and ε_e are often assumed to be both 0.1, but several lines of arguments are against this assumption (e.g., [Fransson & Björnsson 1998](#); [Björnsson & Fransson 2004](#); [Maeda 2012](#); [Soderberg et al. 2012](#); [Kamble et al. 2016](#); [Kundu et al. 2017](#)). In the previous studies of SN Ia radio observations (e.g., [Chomiuk et al. 2012](#); [Pérez-Torres et al. 2014](#); [Kundu et al. 2017](#)), the combination of $(\varepsilon_B, \varepsilon_e) = (0.01, 0.1)$ is also investigated. [Maeda \(2012\)](#) proposed lower values for both ε_B and ε_e by fitting the radio and X-ray observations of well-observed SN Iib 2011dh and the best parameter estimate suggested is $(\varepsilon_B, \varepsilon_e) = (0.006, 0.05)$. We also adopted this combination in Fig. 1. [Björnsson & Fransson \(2004\)](#) and [Kamble et al. \(2016\)](#) also suggest similarly small values for SN Ic 2002ap and SN Iib 2013df, respectively. Because the shock microphysics does not depend on SN types, this estimate should be applicable in SNe Ia as well.

The progenitor systems in the optically thick wind phase at the time of the explosion are mostly excluded in all the microphysics assumption as found in the previous studies (e.g., [Chomiuk et al. 2012](#)). The progenitor systems at the stable He-shell burning phase are mostly excluded if we assume $(\varepsilon_B, \varepsilon_e) = (0.1, 0.1)$. However, this combination is not likely and we argue that the remaining two combinations of ε_B and ε_e provide more realistic constraints when we take the aforementioned parameter constraints from core-collapse SN observations into account. In this case, a large fraction of the systems at the stable He-shell burning are not excluded by the radio observations of SN 2011fe and SN 2014J. All the systems at the weak He-shell flash phase at the time of the explosion are not excluded under the probable microphysics assumptions.

Population synthesis models generally predict that the prompt SNe Ia are dominated by the He star donor channel (e.g., [Wang et al. 2009b](#); [Ruiter et al. 2009](#); [Claeys et al. 2014](#); [Liu et al. 2015a](#)). SN 2014J has been suggested to be a prompt SN Ia ([Nielsen et al. 2014](#)) and it showed unexpectedly early gamma-ray emission from the ^{56}Ni decay which might be related to He accretion from its companion ([Diehl et al. 2014](#)). Although SN 2011fe did not have He star donor signatures, it appeared in a spiral arm of a star-forming galaxy (e.g., [Li et al. 2011](#)) so it might also be from the prompt SN Ia population. Being prompt SNe Ia, both SN 2011fe and SN 2014J may have had a He star donor. In addition, the magnitude limits for the companion stars of SN 2011fe and SN 2014J obtained by the pre-SN images do not exclude a large fraction of He star donors predicted by the population synthesis model. Fig. 3 shows the CSM properties of SN Ia progenitor systems that have the He donor stars below the upper limit of SN 2011fe in Fig. 2. We can see that most systems avoid the constraints from the radio observations. Especially, a major fraction of SNe Ia from the He star donor are predicted to be in the weak He-shell flash phase (Section 4.3) and most of the progenitor systems in this phase are not excluded by the pre-SN images. These systems originate from a wide variety of the initial WD mass,

Table 1. Galactic SN Ia rates from the He star donor channel.

| | rate (10^{-3} yr^{-1}) | |
|-----------------------------------|------------------------------------|-----------------------------------|
| | $\alpha_{\text{CE}}\lambda = 0.5$ | $\alpha_{\text{CE}}\lambda = 1.5$ |
| total | 1.07 | 1.10 |
| stable He-shell burning | 0.25 (23%) | 0.59 (54%) |
| weak He-shell flash | 0.82 (77%) | 0.51 (46%) |
| optically thick wind ^a | 0.11 | 0.11 |

^a AIC progenitors.

Table 2. Galactic SN Ia rates from the He star donor channel having the He companion stars fainter than the SN 2011fe limit as in Fig. 2.

| | rate (10^{-3} yr^{-1}) | |
|-----------------------------------|------------------------------------|-----------------------------------|
| | $\alpha_{\text{CE}}\lambda = 0.5$ | $\alpha_{\text{CE}}\lambda = 1.5$ |
| total | 0.53 | 0.28 |
| stable He-shell burning | 0.15 (30%) | 0.14 (54%) |
| weak He-shell flash | 0.35 (70%) | 0.13 (46%) |
| optically thick wind ^a | 0.03 | 0.01 |

^a AIC progenitors.

He star donor mass, and initial orbital period (cf. Fig. 4). In summary, the current radio observations and pre-explosion images leave many possible systems for the He star donor channel in both SN 2014J and SN 2011fe. We note that subdwarf B star companions are also suggested to avoid these observational constraints (?).

4.2 SN 2012Z

A possible He companion star at the explosion site of SN Iax 2012Z is discovered ([McCully et al. 2014](#)). We show this candidate companion star property in Fig. 2. The effective temperature is estimated by its color by assuming the relation provided by [Torres \(2010\)](#). We marked 3 models that are consistent with this possible companion star in Fig. 2 as well as in Fig. 1. They all have the initial He donor mass of $1.05 M_{\odot}$ and their initial orbital periods are $1.8 - 2.0$ days. The initial WD mass is $1.2 M_{\odot}$. The final He donor mass is $0.86 M_{\odot}$ with the final orbital periods of $1.9 - 2.1$ days. The WD accretion rate at the time of the explosion is $\approx 10^{-6} M_{\odot} \text{ yr}^{-1}$. These models are in the stable He-shell burning phase and have relatively high CSM density (Fig. 1). However, [Liu et al. \(2015b\)](#) found that such a progenitor system for SN 2012Z is rather rare. We refer to [Liu et al. \(2015b\)](#) for the further investigation of SNe Iax from the He-star donor channel.

4.3 Rates

[Wang et al. \(2009b\)](#) estimated Galactic SN Ia rates from each He star donor progenitor system based on the binary evolution models of [Wang et al. \(2009a\)](#). Their results are summarized in Table 1. [Wang et al. \(2009b\)](#) adopted the rapid binary evolution code by [Hurley et al. \(2000, 2002\)](#)

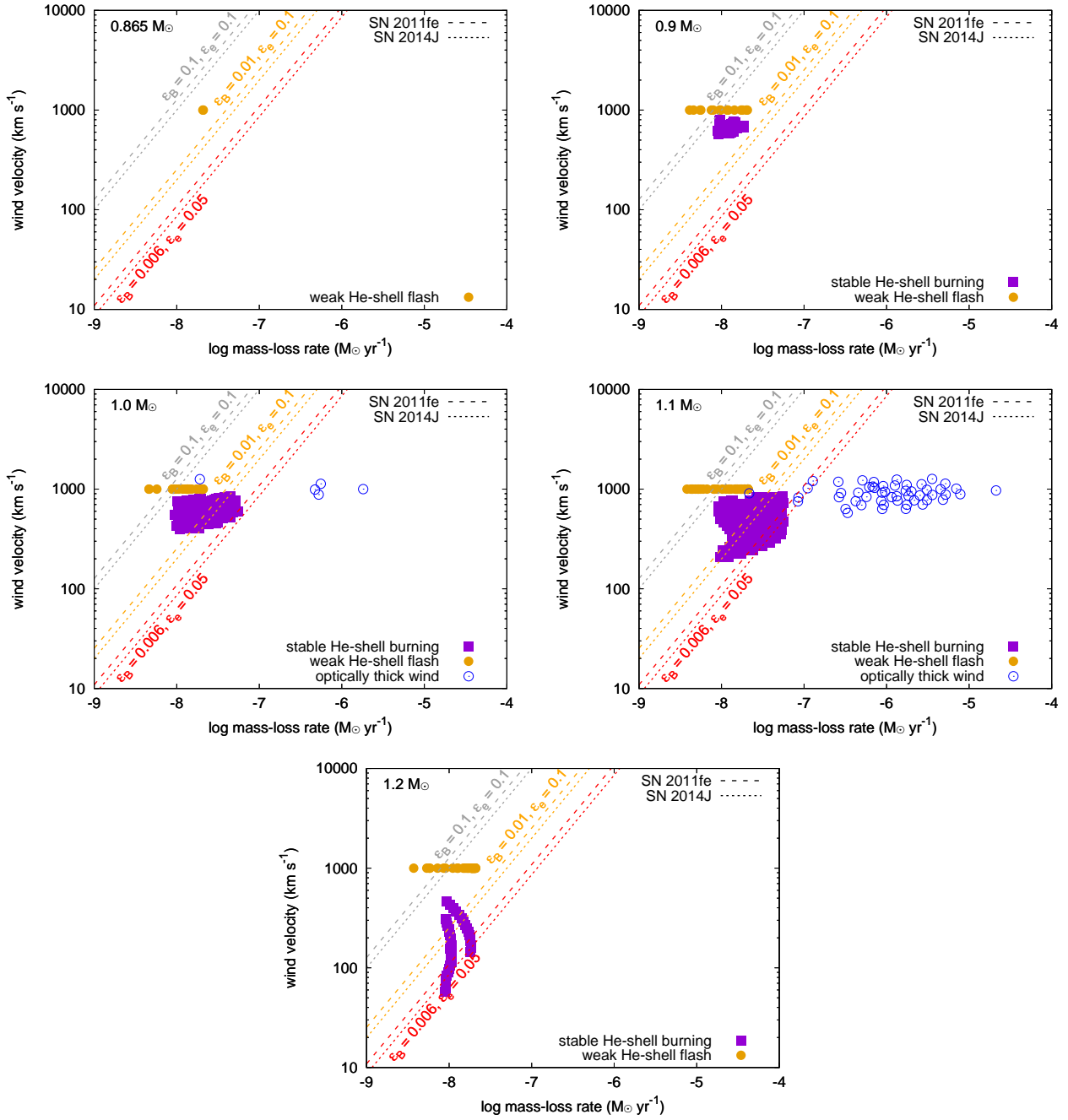


Figure 4. CSM properties of SNe Ia from the He star donor channel with different initial WD masses. The initial WD masses are shown at the top right of each panel. See Fig. 1 for further details.

for their population synthesis. When a WD + He star system is in the parameter range for SN Ia progenitors obtained by Wang et al. (2009a) at the onset of the Roche-lobe overflow, the system is assumed to produce a SN Ia. We assume that the systems at the optically thick wind phase when the WD reaches $1.378 M_{\odot}$ undergo AIC instead of SNe Ia. An important but uncertain parameter of the binary population synthesis in estimating the SN Ia rates is $\alpha_{CE}\lambda$, where α_{CE} is the common-envelope ejection efficiency and λ is the envelope binding energy parameter (Dewi & Tauris 2000; Tauris & Dewi 2001). The two parameters, i.e., $\alpha_{CE}\lambda = 0.5$

and 1.5 are adopted to estimate the SN Ia rate from the He star channel.

The total Galactic SN Ia rate from the He star donor channel is estimated to be $\approx 1.1 \times 10^{-3} \text{ yr}^{-1}$ in both $\alpha_{CE}\lambda = 0.5$ and $\alpha_{CE}\lambda = 1.5$ cases. However, the fraction of the progenitor systems in each phase depends strongly on the assumed $\alpha_{CE}\lambda$ as summarized in Table 1. With $\alpha_{CE}\lambda = 0.5$, the progenitor system in the weak He-shell flash phase dominates SNe Ia with He star donors, but both systems in the weak He-shell flash phase and the stable He-shell burning phase almost equally contribute to SNe Ia when $\alpha_{CE}\lambda = 1.5$.

We note that $\alpha_{\text{CE}}\lambda$ is constrained to be around 0.1 – 1 in low- and intermediate-mass stars (e.g., Zorotovic et al. 2010; De Marco et al. 2011; Davis et al. 2012) so the systems in the weak He-shell flash may be more common in SNe Ia from He star donors.

We showed that many systems from the He star donor channel avoid the detection limit of the SN 2011fe progenitor system in Section 4.1. Table 2 shows the SN Ia rates only for these systems avoiding the SN 2011fe limit. We find about a half of SNe Ia from this channel have a He companion star fainter than the SN 2011fe limit in the case of $\alpha_{\text{CE}}\lambda = 0.5$, while about 30% of the systems avoid the limit in the case of $\alpha_{\text{CE}}\lambda = 1.5$.

4.4 Initial WD mass dependence

A wide range of initial WD masses is adopted in the binary evolution model of Wang et al. (2009a). Fig. 4 shows the CSM properties with different initial WD masses. The majority of the progenitor systems have the initial WD mass of $1.1 M_{\odot}$ regardless of the phases at the time of the explosions. No clear dependence of the CSM properties on the initial WD mass exists and it is difficult to constrain the initial WD mass through radio observations.

4.5 Uncertainties

We have adopted the binary stellar evolution model of Wang et al. (2009a) in this study. However, it should be kept in mind that uncertainties in the stellar evolution calculations can affect the expected CSM properties presented in this work. For example, the WD mass growth rates under given accretion rates are still uncertain (e.g., Brooks et al. 2016; Wong & Schwab 2019). Different mass-retention efficiencies onto a WD are expected to affect the results of our binary calculations (e.g., Bours et al. 2013; Ruiter et al. 2013). In addition, rotation of WDs is ignored in the stellar evolution model we adopted, which can also change the WD evolution (Hachisu et al. 2012). A spin-down process could be important to determine the moment of the SN explosions if rotation of WDs is considered. Depending on the spin-down timescale, the CSM around the progenitor system could diffuse and reach a density similar to that of the interstellar medium, leading to the lack of radio emission (Justham 2011). Observations of the radio emission from SNe Ia with the He star donor channel would give us a better understanding of these uncertainties.

4.6 Future prospects

We have shown that the current radio observations are not deep enough to exclude most of the He star donor channel of the SD model. It will be necessary to conduct radio observations of nearby SNe Ia like SN 2011fe and SN 2014J with deeper limits to detect radio emission from SN Ia from the He star donor channel. For this purpose, Five hundred meter Aperture Spherical radio Telescope (FAST) will shortly be a powerful tool. The upper limits of the radio emission from SN 2011fe and SN 2014J were $\sim 10 \mu\text{Jy}$ (Chomiuk et al. 2016) at ~ 1 GHz. FAST is expected to reach $\sim 1 \mu\text{Jy}$ at ~ 1 GHz in a few hours and can make the flux limit deeper

by one order of magnitude. With this depth, a large fraction of SNe Ia from the He star donor channel especially in the stable He-shell burning phase are predicted to be detectable (Fig. 1). Square Kilometer Array (SKA) will eventually allow us to observe SNe Ia down to $\sim 0.1 \mu\text{Jy}$ (Perez-Torres et al. 2015) and we should be able to make the final conclusion on the He star donor channel.

There are several other suggested ways to test the He star donor SD channel. For example, the SN ejecta are predicted to strip the surface of the He star donors and the SN ejecta will be contaminated by the stripped He (Pan et al. 2010, 2012; Liu et al. 2013). The amount of He stripped by the SN ejecta is predicted to be $\sim 0.01 M_{\odot}$ (Pan et al. 2010, 2012; Liu et al. 2013). The SN ejecta contaminated by the stripped He are predicted to have He emission in the nebular phase (Botyánszki et al. 2018). No He emission is observed from SN 2011fe and SN 2014J in the nebular phase and the stripped mass is constrained to be less than $\sim 0.01 M_{\odot}$ (Tucker et al. 2019). SN 2012Z, which is suggested to have a He star companion from the pre-explosion image (McCully et al. 2014), however, did not show the predicted He emission and the stripped mass is also constrained to be less than $\sim 0.01 M_{\odot}$ (Tucker et al. 2019). The predicted masses and the upper limits are now comparable and it is still difficult to make a firm conclusion on the mass stripping with the current observations. Further late-phase observations of SNe Ia are required.

Another intriguing prediction is that the He star donor may get brighter in $\sim 10 - 100$ years after the explosion because of the heat provided by the SN ejecta collision (Pan et al. 2013). Especially for the case of SN 2011fe, the faint He star donor that was not detected by the pre-explosion image could be now bright enough to be detected (Pan et al. 2013). This prediction could also be tested by SN 2012Z with the He star companion (McCully et al. 2014).

5 CONCLUSIONS

We have investigated the CSM properties around SN Ia progenitors from the SD model having a He star donor. We estimated the CSM properties based on the binary evolution calculations of WD + He star systems by Wang et al. (2009a). The binary evolution calculations suggest that SNe Ia from the He star donor channel occur during the stable He-shell burning phase or the weak He-shell flash phase. We found that the current deepest radio observations from SN 2011fe and SN 2014J cannot exclude the possibilities of SN Ia progenitors with He star donors in either phase (Fig. 1). We also found that their pre-explosion images cannot exclude most of the progenitor system in the weak He-shell flash phase, which is predicted to dominate SNe Ia with He star donors (Fig. 2). Therefore, both SN 2011fe and SN 2014J could both be prompt SNe Ia. Future radio observations by FAST and SKA are likely to detect radio emission from the CSM interaction in SNe Ia from the He star donor channel if a SN Ia occurs as close as SN 2011fe or SN 2014J.

ACKNOWLEDGEMENTS

We thank the referee for a constructive report. TJM thanks Sunny Wong for comments. TJM is supported by the Grants-in-Aid for Scientific Research of the Japan Society for the Promotion of Science (JP17H02864 and JP18K13585). BW is supported by the National Natural Science Foundation of China (Nos 11873085, 11673059 and 11521303), the Chinese Academy of Sciences (No QYZDB-SSW-SYS001), and the Yunnan Province (No 2018FB005). ZWL is supported by the National Natural Science Foundation of China (NSFC, No. 11873016) and 100 Talents Programme of the Chinese Academy of Sciences.

REFERENCES

- Bildsten L., Shen K. J., Weinberg N. N., Nelemans G., 2007, *ApJ*, **662**, L95
- Björnsson C.-I., Fransson C., 2004, *ApJ*, **605**, 823
- Bloom J. S., et al., 2012, *ApJ*, **744**, L17
- Botyánszki J., Kasen D., Plewa T., 2018, *ApJ*, **852**, L6
- Bours M. C. P., Toonen S., Nelemans G., 2013, *A&A*, **552**, A24
- Brooks J., Bildsten L., Schwab J., Paxton B., 2016, *ApJ*, **821**, 28
- Chandler C. J., Marvil J., 2014, *The Astronomer's Telegram*, **5812**
- Chevalier R. A., 1998, *ApJ*, **499**, 810
- Chevalier R. A., Fransson C., 2006, *ApJ*, **651**, 381
- Chomiuk L., et al., 2012, *ApJ*, **750**, 164
- Chomiuk L., Zauderer B. A., Margutti R., Soderberg A., 2014, *The Astronomer's Telegram*, **5800**
- Chomiuk L., et al., 2016, *ApJ*, **821**, 119
- Claeys J. S. W., Pols O. R., Izzard R. G., Vink J., Verbunt F. W. M., 2014, *A&A*, **563**, A83
- Dan M., Rosswog S., Brüggen M., Podsiadlowski P., 2014, *MNRAS*, **438**, 14
- Davis P. J., Kolb U., Knigge C., 2012, *MNRAS*, **419**, 287
- De Marco O., Passy J.-C., Moe M., Herwig F., Mac Low M.-M., Paxton B., 2011, *MNRAS*, **411**, 2277
- Deufel B., Barwig H., Šimić D., Wolf S., Drory N., 1999, *A&A*, **343**, 455
- Dewi J. D. M., Tauris T. M., 2000, *A&A*, **360**, 1043
- Diehl R., et al., 2014, *Science*, **345**, 1162
- Eggleton P. P., 1971, *MNRAS*, **151**, 351
- Eggleton P. P., 1972, *MNRAS*, **156**, 361
- Eggleton P. P., 1973, *MNRAS*, **163**, 279
- Foley R. J., et al., 2013, *ApJ*, **767**, 57
- Fransson C., Björnsson C.-I., 1998, *ApJ*, **509**, 861
- Hachisu I., Kato M., Nomoto K., 1996, *ApJ*, **470**, L97
- Hachisu I., Kato M., Nomoto K., 2012, *ApJ*, **756**, L4
- Han Z., Podsiadlowski P., Eggleton P. P., 1994, *MNRAS*, **270**, 121
- Han Z., Tout C. A., Eggleton P. P., 2000, *MNRAS*, **319**, 215
- Horesh A., et al., 2012, *ApJ*, **746**, 21
- Hoyle F., Fowler W. A., 1960, *ApJ*, **132**, 565
- Huang R.-q., Yu K. N., 1996, *Chinese Astron. Astrophys.*, **20**, 175
- Hurley J. R., Pols O. R., Tout C. A., 2000, *MNRAS*, **315**, 543
- Hurley J. R., Tout C. A., Pols O. R., 2002, *MNRAS*, **329**, 897
- Iben Jr. I., Tutukov A. V., 1984, *ApJS*, **54**, 335
- Iben Jr. I., Tutukov A. V., 1994, *ApJ*, **431**, 264
- Justham S., 2011, *ApJ*, **730**, L34
- Kamale A., et al., 2016, *ApJ*, **818**, 111
- Kato M., Hachisu I., 1994, *ApJ*, **437**, 802
- Kato M., Hachisu I., 2004, *ApJ*, **613**, L129
- Kelly P. L., et al., 2014, *ApJ*, **790**, 3
- Kundu E., Lundqvist P., Pérez-Torres M. A., Herrero-Illana R., Alberdi A., 2017, *ApJ*, **842**, 17
- Li W., et al., 2011, *Nature*, **480**, 348
- Liu Z.-W., et al., 2013, *ApJ*, **774**, 37
- Liu Z.-W., Moriya T. J., Stancliffe R. J., Wang B., 2015a, *A&A*, **574**, A12
- Liu Z.-W., Stancliffe R. J., Abate C., Wang B., 2015b, *ApJ*, **808**, 138
- Liu D., Wang B., Han Z., 2018, *MNRAS*, **473**, 5352
- Livio M., Mazzali P., 2018, *Phys. Rep.*, **736**, 1
- Maeda K., 2012, *ApJ*, **758**, 81
- Maeda K., Terada Y., 2016, *International Journal of Modern Physics D*, **25**, 1630024
- Maoz D., Mannucci F., Nelemans G., 2014, *ARA&A*, **52**, 107
- McCully C., et al., 2014, *Nature*, **512**, 54
- Mori K., Famiano M. A., Kajino T., Kusakabe M., Tang X., 2019, *MNRAS*, **482**, L70
- Moriya T. J., Groh J. H., Meynet G., 2013, *A&A*, **557**, L2
- Neunteufel P., Yoon S. C., Langer N., 2019, arXiv e-prints, p. arXiv:1904.12421
- Nielsen M. T. B., Gilfanov M., Bogdán Á., Woods T. E., Nelemans G., 2014, *MNRAS*, **442**, 3400
- Nomoto K., 1982a, *ApJ*, **253**, 798
- Nomoto K., 1982b, *ApJ*, **257**, 780
- Nomoto K., Iben Jr. I., 1985, *ApJ*, **297**, 531
- Nomoto K., Kondo Y., 1991, *ApJ*, **367**, L19
- Nugent P. E., et al., 2011, *Nature*, **480**, 344
- Pakmor R., Kromer M., Taubenberger S., Sim S. A., Röpke F. K., Hillebrandt W., 2012, *ApJ*, **747**, L10
- Pan K.-C., Ricker P. M., Taam R. E., 2010, *ApJ*, **715**, 78
- Pan K.-C., Ricker P. M., Taam R. E., 2012, *ApJ*, **750**, 151
- Pan K.-C., Ricker P. M., Taam R. E., 2013, *ApJ*, **773**, 49
- Pérez-Torres M. A., et al., 2014, *ApJ*, **792**, 38
- Pérez-Torres M., et al., 2015, *Advancing Astrophysics with the Square Kilometre Array (AASKA14)*, p. 60
- Perlmutter S., et al., 1999, *ApJ*, **517**, 565
- Pols O. R., Tout C. A., Eggleton P. P., Han Z., 1995, *MNRAS*, **274**, 964
- Pols O. R., Schröder K.-P., Hurley J. R., Tout C. A., Eggleton P. P., 1998, *MNRAS*, **298**, 525
- Riess A. G., et al., 1998, *AJ*, **116**, 1009
- Ruiter A. J., Belczynski K., Fryer C., 2009, *ApJ*, **699**, 2026
- Ruiter A. J., et al., 2013, *MNRAS*, **429**, 1425
- Saio H., Nomoto K., 1985, *A&A*, **150**, L21
- Sato Y., Nakasato N., Tanikawa A., Nomoto K., Maeda K., Hachisu I., 2016, *ApJ*, **821**, 67
- Shen K. J., 2015, *ApJ*, **805**, L6
- Soderberg A. M., et al., 2012, *ApJ*, **752**, 78
- Stritzinger M. D., et al., 2015, *A&A*, **573**, A2
- Tauris T. M., Dewi J. D. M., 2001, *A&A*, **369**, 170
- Thielemann F.-K., Brachwitz F., Höflich P., Martínez-Pinedo G., Nomoto K., 2004, *New Astron. Rev.*, **48**, 605
- Torres G., 2010, *AJ*, **140**, 1158
- Tucker M. A., et al., 2019, arXiv e-prints,
- Wang B., 2018, *Research in Astronomy and Astrophysics*, **18**, 049
- Wang B., Meng X., Chen X., Han Z., 2009a, *MNRAS*, **395**, 847
- Wang B., Chen X., Meng X., Han Z., 2009b, *ApJ*, **701**, 1540
- Wang B., Podsiadlowski P., Han Z., 2017, *MNRAS*, **472**, 1593
- Webbink R. F., 1984, *ApJ*, **277**, 355
- Whelan J., Iben Jr. I., 1973, *ApJ*, **186**, 1007
- Wong T. L. S., Schwab J., 2019, arXiv e-prints,
- Woosley S. E., Taam R. E., Weaver T. A., 1986, *ApJ*, **301**, 601
- Yamanaka M., et al., 2015, *ApJ*, **806**, 191
- Yaron O., Prialnik D., Shara M. M., Kovetz A., 2005, *ApJ*, **623**, 398
- Yoon S.-C., Langer N., 2003, *A&A*, **412**, L53
- Yoon S.-C., Podsiadlowski P., Rosswog S., 2007, *MNRAS*, **380**, 933
- Zorotovic M., Schreiber M. R., Gänsicke B. T., Nebot Gómez-Morán A., 2010, *A&A*, **520**, A86

This paper has been typeset from a $\text{\TeX}/\text{\LaTeX}$ file prepared by the author.